Published in final edited form as:
Sci Transl Med. 2010 September 29; 2(51): 51ra70. doi:10.1126/scitranslmed.3001599.

Interfering with Resistance to Smoothened Antagonists by Inhibition of the PI3K Pathway in Medulloblastoma

Silvia Buonamici[1,*], **Juliet Williams**[1,#,*], **Michael Morrissey**[1], **Anlai Wang**[1], **Ribo Guo**[1], **Anthony Vattay**[1], **Kathy Hsiao**[1], **Jing Yuan**[1], **John Green**[1], **Beatrice Ospina**[1], **Qunyan Yu**[1], **Lance Ostrom**[1], **Paul Fordjour**[1], **Dustin L. Anderson**[1], **John E. Monahan**[1], **Joseph F. Kelleher**[1], **Stefan Peukert**[1], **Shifeng Pan**[2], **Xu Wu**[2], **Sauveur-Michel Maira**[1], **Carlos Garcia-Echeverria**[1,$], **Kimberly J. Briggs**[3], **D. Neil Watkins**[4], **Yung-mae Yao**[1], **Christoph Lengauer**[1,$], **Markus Warmuth**[1], **William R. Sellers**[1], and **Marion Dorsch**[1]

[1]Novartis Institutes for Biomedical Research, Cambridge, MA 02139, USA and Basel, Switzerland [2]Genomics Institute of the Novartis Research Foundation, San Diego, CA 92121, USA [3]Sidney Kimmel Comprehensive Cancer Centre, Johns Hopkins University, Baltimore, MD 21231, USA [4]Monash Institute of Medical Research, Monash University, Clayton, Victoria, 3168, Australia

Abstract

Mutations in Hedgehog (Hh) pathway genes, leading to constitutive activation of Smoothened (Smo), occur in medulloblastoma. Antagonists of Smo induce tumor regression in mouse models of medulloblastoma and hold great promise for treating this disease. However, acquired resistance has emerged as a challenge to targeted therapeutics and may limit their anti-cancer efficacy. Here, we describe novel mechanisms of acquired resistance to Smo antagonists in medulloblastoma. NVP-LDE225, a potent and selective Smo antagonist, inhibits Hh signaling and induces tumor regressions in allograft models of medulloblastoma that are driven by mutations of Patched (Ptch), a tumor suppressor in the Hh pathway. However, evidence of resistance was observed during the course of treatment. Molecular analysis of resistant tumors revealed distinct resistance mechanisms. Chromosomal amplification of Gli2, a downstream effector of Hh signaling, or more rarely point mutations in Smo led to reactivated Hh signaling and restored tumor growth. Unexpectedly, analysis of pathway gene-expression signatures selectively deregulated in resistant tumors identified increased phosphoinositide 3-kinase (PI3K) signaling as another potential resistance mechanism. Probing the functional relevance of increased PI3K signaling, we demonstrated that the combination of NVP-LDE225 with the PI3K class I inhibitor NVP-BKM120 or the dual PI3K/mTOR inhibitor NVP-BEZ235 markedly delayed the development of resistance. Our findings have important clinical implications for future treatment strategies in medulloblastoma.

Corresponding author: marion.dorsch@novartis.com, 617-871-3942.
[#]Present address: Cancer Research Technology, Gower Street, London WC1E 6BT, UK.
[$]Present address: Sanofi-Aventis, 13 Quai Jules Guesde, 94403 Vitry-sur-Seine, France.
[*]These authors contributed equally to this work.

Author contributions: M.D. conceived and directed the project. S.B., J.W., Y.Y., R.G., J.Y. and J.G. designed, executed and analyzed pharmacology studies. M.D., J.F. K., X.W., A.W., A.V. and K.H. designed and carried out cellular and biomarker studies. Genomic profiling studies were designed and analyzed by M.M., J.M., P.F., D.L.A. and L.O. S.P. and St.P. directed the Smo antagonist chemistry. S.M. and C.G.E. provided NVP-BEZ235 and input to study design. K.J.B. and D.N.W. provided the *Ptch*$^{+/-}$*Hic*$^{+/-}$ model. C.L., M.W. and W.R.S. provided input into experimental designs. M.D., S.B. and W.R.S. wrote the manuscript.

Competing interests: The majority of the authors are employees of Novartis Pharmaceuticals.

Introduction

The Hh pathway plays a critical role in the development and homeostasis of many organs and tissues. In the resting state, the Hh receptor Ptch inhibits the activity of Smo, a G protein-coupled (GPCR)-like molecule. Upon Hh ligand binding, Ptch inhibition is attenuated, and Smo signals via a cytosolic complex of proteins leading to activation of the Gli family of transcription factors (1). Gli1 and Gli2 are responsible for most transcriptional activator functions, whereas Gli3 acts mainly as a repressor. Gli1 is a direct transcriptional target of Hh signaling and a marker for pathway activity. Loss of function mutations in Ptch or gain of function mutations in Smo leading to ligand-independant pathway activation of Smo have been identified in medulloblastoma and basal cell carcinoma (2). Mice with a hetrozygous deletion of Ptch develop medulloblastomas that are highly responsive to Smo antagonists (3) strongly suggesting the "addiction" of these tumors to Smo activity. Importantly, the extent of tumor cell addiction to oncogenic pathways can be most robustly revealed by understanding the mechanisms of emergent resistance following treatment of genetically defined cancers with targeted therapeutics (4). To understand the key oncogenic mechanisms operant in the setting of Ptch deficiency, we have explored mechanisms of resistance to Smo inhibitors using NVP-LDE225, a novel Smo antagonist currently in clinical development.

Results

Emergence of resistance to Smo inhibition

NVP-LDE225 is a potent and selective oral Smo antagonist from a novel structural class (Supplementary Fig. 1)(5). This molecule displaces the binding of the synthetic Smo Agonist 1.5 (6) to human and mouse Smo with an IC_{50} of 11 and 12 nM, respectively, and in low nanomolar concentrations inhibits Hh-signaling in human and mouse cells (Supplementary Table 1) (5). In medulloblastoma tumors derived from *Ptch*$^{+/-}$*p53*$^{-/-}$ mice (7) and implanted into nude mice, expression of the Hh pathway target gene *Gli1* was completely suppressed by the oral administration of 20 mg/kg/day qd of NVP-LDE225 (Fig. 1A). Consistent with the dose-response for suppression of Gli1 mRNA (data not shown), treatment of tumor-bearing mice with NVP-LDE225 induced partial growth inhibition at 10 mg/kg/day and near complete regressions (84 to 92%) beginning at doses of 20 mg/kg/day (Fig. 1B). However, on day 13 of continuous dosing of NVP-LDE225 tumor re-growth was observed in all treatment groups indicating the development of resistance. Resistant tumors had a more heterogenous histological appearance compared to sensitive tumors (Supplementary Fig. 2). The development of resistance was also seen in mice treated with HhAntag (Fig. 1B)., a Smo antagonist from a structurally distinct class (8).

Although complete suppression of *Gli1* mRNA in response to initial NVP-LDE225 treatment was seen, re-expression of *Gli1* mRNA was observed in resistant tumors (Fig. 1A). A similar pattern of re-expression in resistant tumors was observed for several Hh pathway target genes such as *Ptch1*, *Ptch2* and *CyclinD1 (2)* (Supplementary Fig. 3A). These data show that acquired resistance to Smo inhibition is associated with reactivation of Hh signaling.

To determine whether resistance and Gli1 reactivation was unique to the *Ptch*$^{+/-}$*p53*$^{-/-}$ model, similar experiments were carried out using allografts derived from *Ptch*$^{+/-}$*Hic1*$^{+/-}$ mice (9). *Hypermethylated in Cancer-1 (Hic1)* is a frequent target of epigenetic gene silencing in medulloblastoma (9). In the context of a *Ptch*$^{+/-}$ background, heterozygous deletion of *Hic1* leads to the development of Hh-pathway dependant medulloblastoma. Thus, nude mice were implanted subcutaneously with medulloblastomas derived from *Ptch*$^{+/-}$*Hic1*$^{+/-}$ mice and treated with NVP-LDE225 orally at similar doses and schedules.

Pronounced inhibition of *Gli1, Ptch1*, *Ptch2* and *CyclinD1* mRNA expression (Supplementary Fig. 4A and 5) and tumor regression (Supplementary Fig. 4B) were observed during initial treatment, followed by re-growth of some tumors (Supplementary Table 2) that had restored a variable degree of Hh pathway target gene expression *1* expression (Supplementary Fig. 4A and 5). Similar observations were made in the $Ptch^{+/-}$ allograft model (data not shown). The rapid emergence of resistance to NVP-LDE225 with restoration of Hh pathway target gene expression expression in both models is consistent with a marked addiction to Hh signaling in $Ptch^{+/-}$ medulloblastoma. To confirm that NVP-LDE225 resistance resulted from a cell autonomous rather than an extrinsic mechanism such as decreased drug exposure, the ex-vivo proliferation (10) of tumor cells freshly isolated from sensitive (pre-treatment) and resistant tumors was measured in response to NVP-LDE225. Whereas growth of sensitive medulloblastoma cells was robustly inhibited (IC_{50} 6 nM), growth of resistant tumor cells was largely unaffected by exposure to NVP-LDE225 (IC_{50} >20 μM) (Fig. 1C) or to other Smo antagonists such as HhAntag and cyclopamine (Supplementary Table 3). Together these data suggested that cell autonomous mechanisms caused resistance to Smo inhibition in these tumors.

Re-activation of Hh signaling in resistant tumors

Next, we took an unbiased approach to the discovery of potential resistance mechanisms. Specifically, expression profiles of $Ptch^{+/-}p53^{-/-}$ tumors were obtained using Affymetrix murine gene expression arrays, and were queried in a hypothesis-directed mode for signatures corresponding to a pattern of expression that was down-regulated upon short-term treatment with NVP-LDE225, but re-expressed in resistant tumors (Fig. 2A). Genes ordered by Spearman rank correlation with this pattern are shown in Fig. 2B and C. *Gli1* emerged as the top ranking gene, closely followed by *CyclinD1*, *Ptch1* and *Hhip*, three bona fida Hh pathway target genes (2). Using a Fisher's Exact Test to probe gene-sets extracted from GeneGo Metacore database (11), the top ranked genes were shown to be enriched in the transcriptional targets of Gli2 (p=0.001, false discovery rate (FDR)=0.04) and Gli1 (p=0.003, FDR=0.08). Sensitive and resistant tumors from the $Ptch^{+/-}Hic1^{+/-}$ model were subjected to the same analysis and also showed significant regulation of Gli2 (p=0.006) and Gli1 (p=0.04) target genes. In aggregate, these data confirm and expand on our initial observation that Hh signaling is reactivated in resistant tumors.

Smo mutations in resistant tumors

Resistance to inhibitors of BCR-ABL, c-KIT and EGFR1 kinases is most often ascribed to the development of mutations in the direct drug target (4). In addition, recently a mutation in *Smo* was described as mechanism of resistance to the Smo inhibitor GDC0449 (12). To determine whether point mutations in *Smo* might account for resistance to NVP-LDE225 and Gli reactivation in both medulloblastoma models, genomic DNA isolated from resistant tumors was subjected to PCR-based amplification and sequencing of all coding *Smo* exons. Surprisingly, missense point mutations in *Smo* were detected in only seven out of 135 resistant tumors, resulting in changes of leucine 225 to arginine (L225R), asparagine 223 to aspartic acid (N223D), serine 391 to asparagine (S391N), aspartic acid 388 to asparagine (D388N) and glycine 475 to serine (G457S) (Table 1 and Supplementary Fig. 6). All five mutations differ from the previously described aspartic acid 477 to glycine (D477G) mutation (12) but similarly abrogate or decrease Smo inhibition by NVP-LDE225 (Table 1 and Supplementary Fig. 7). Importantly these data suggest that nucleotide-based mutations in Smo are not a dominant driver of resistance to NVP-LDE225.

Gli2 amplifications in resistant tumors

To determine whether other genetic abnormalities including chromosomal alterations might account for resistance to Smo inhibition, genomic DNA isolated from three sensitive and

three resistant *Ptch*$^{+/-}$*p53*$^{-/-}$ tumors was subjected to genome-wide array-based comparative genomic analysis (aCGH). Two of the three resistant tumors showed a focal amplification of a region on chromosome 1 (1qE2-4) containing *Gli2* (Fig. 2D). Next, copy number variations in *Gli1, 2 and 3* was determined by quantitative PCR in a larger set of resistant tumor samples. This analysis revealed *Gli2* amplification in 50% of *Ptch*$^{+/-}$*p53*$^{-/-}$ (Fig 2E) and 20% of *Ptch*$^{+/-}$ resistant tumors (data not shown), but not in sensitive tumors, nor in any of the *Ptch*$^{+/-}$*Hic*$^{+/-}$ resistant tumors. No copy number changes for *Gli1* and *Gli3* were detected (data not shown). Gli2 amplifications appeared to be less frequent at higher doses but larger sample numbers will be required to draw a firm conclusion. In keeping with the notion that amplification would result in up-regulation of *Gli2* mRNA levels, we found a strong correlation between expression and amplification where *Gli2* mRNA expression was increased 2- to 20-fold in *Gli2*-amplified resistant tumors compared to sensitive tumors (Fig. 2F). A small number of resistant tumors demonstrated elevated *Gli2* mRNA expression in the absence of clear amplification, suggesting that alternative mechanisms may also lead to *Gli2* mRNA up-regulation. In the *Ptch*$^{+/-}$*Hic*$^{+/-}$ model, *Gli2* expression was not elevated compared to sensitive tumors (Suppl. Fig. 5B)

The functional significance of *Gli2* amplification was investigated in freshly isolated cells from a *Gli2*-amplified and *Gli2* overexpressing, NVP-LDE225-resistant tumor transfected with *Gli2* siRNA. As shown in Fig. 2G, treatment with *Gli2* siRNAs resulted in a 50% to 70% knock-down of *Gli2* mRNA. This was correlated with inhibition of proliferation, and also led to the suppression of *Gli1* mRNA, a well defined transcriptional target of Gli2 (13). Moreover, preliminary data indicated that knock-down of *Gli2* resulted in the partial reconstitution of sensitivity to NVP-LDE225. The IC_{50} for growth inhibition for NVP-LDE225 shifted from >20 uM to 0.1 μM in the presence of *Gli2* knock-down (data not shown). These data show that Gli2 is a critical effector of tumor cell growth downstream of mutations in the *Ptch* receptor, and can act as a mediator of resistance to Smo inhibitors.

Upregulation of Igf-R/PI3K signaling in resistant tumors

Gli2 amplification was frequent in resistant tumors, however it was not uniform. Furthermore, *Gli2* amplifications were not detected in *Ptch*$^{+/-}$*Hic1*$^{+/-}$ resistant tumors, suggesting that tumors may escape Smo inhibition through alternative routes. To search for such a mechanism, we probed the *Ptch*$^{+/-}$*p53*$^{-/-}$ medulloblastoma expression dataset with an expression vector emphasizing the emergence of new or up-regulated pathways not regulated by short-term treatment with NVP-LDE225 (Fig. 3A). We created a rank-ordered list of genes differentially expressed (by t-test) between resistant tumors and all other tumors (control and treated sensitive), and reapplied the previously-described gene-set analysis in order to detect signaling pathways preferentially enriched during the emergence of resistance (Fig. 3B, C and Supplementary Table 4).

Strikingly, in this analysis three of the most highly ranked pathways (Akt, PIP3 and Igf-1R) were directly related to Igf-1R/PI3K signaling (Fig. 3B), strongly suggesting that a compensatory upregulation of PI3K/mTor signaling might contribute to development of resistance. Intriguingly, this mechanism of resistance has been observed previously with EGFR inhibitors (4).

The 29-gene PI3K gene-set in Fig. 3C derived from the Akt, PIP3 and Igf-1R pathway category was surveyed across an additional 3 vehicle (sensitive) and 16 resistant *Ptch*$^{+/-}$*p53*$^{-/-}$ tumors (Supplementary Fig 8). The “PI3K signature score” of each tumor, defined as the average z-score of all genes in the 29-gene set, was upregulated ($p<0.01$) in 11/16 resistant tumors but not in the three sensitive tumors. Gli2 amplification and Smo mutation were detected in 6/16 and 1/16 resistant tumors, respectively. Upregulation of the PI3K signature was detected in tumors with and w/o Gli2 amplification.

To address the functional relevance of the PI3K upregulation, we asked whether a combination of NVP-LDE225 with the PI3K class I inhibitor NVP-BKM120 could block the development of resistance. Following continuous treatment with NVP-LDE225, tumors derived from the *Ptch*$^{+/-}$*p53*$^{-/-}$ model regressed but then started to re-grow as seen previously (Fig. 3D and E). However, the combination of NVP-LDE225 and NVP-BKM120 delayed tumor re-growth. NVP-BKM120 as single agent, on the other hand, had no effect on tumor growth. Western blot analysis of tumors from different treatment group demonstrated increased PI3K/mTor pathway activation in resistant tumors as measured by phosphorylation of S6 and 4EBP1 and its inhibition in tumors treated with NVP-BKM120 or the combination (Fig. 3I).

We expanded our studies to the *Ptch*$^{+/-}$*Hic*$^{+/-}$ model that lacked *Gli2* amplifications but similarly to the *Ptch*$^{+/-}$*p53*$^{-/-}$ demonstrated upregulation of the PI3K/mTor pathway in resistant tumors (Supplementary Table 5). Combination treatment of *Ptch*$^{+/-}$*Hic*$^{+/-}$ tumors with NVP-LDE225 and the dual PI3K/mTor inhbitor NVP-BEZ235 resulted in a marked delay of tumor re-growth compared to treatment with single agent NVP-LDE225 (Fig. 4A and B). Moreover, while only 1 complete regression was observed after 61 days of treatment in the group treated with NVP-LDE225 alone, 5 complete regresssions were observed in the combination group (Supplementary table 6). Similar results were obtained following treatment of NVP-LDE225 in combination with the mTOR inhibitor RAD001 (Supplementary Fig. 9A and B). In keeping with these data PI3K/mTor pathway activation as measured by S6 and 4EBP1 phosphorylation was up-regulated in resistant tumors and was inhibited in tumors treated with NVP-BEZ235 (Fig. 4C) or RAD001 (Supplementary Fig. 9C).

In summary, our data in two different models of medulloblastoma using three different inhibitors of the PI3K/mTor pathway provide a very strong rationale that the combination of Smo antagonists with PI3K/mTor inhibitors may delay or prevent the development of resistance to Smo inhibitors in medulloblastoma.

Discussion

Several Smo antagonists including NVP-LDE225 are currently being evaluated in clinical trials in patients with advanced solid tumors including medulloblastoma (16). However, acquired resistance has emerged as a challenge to targeted therapeutics and may limit their anti-cancer efficacy (4). Indeed, evidence of resistance to Smo inhibition has recently been reported in a medulloblastoma patient who progressed during therapy with the Smo antagonist GDC0449 (17).

Here, we describe our efforts to identify novel mechanisms of acquired resistance to Smo antagonists in *Ptch*$^{+/-}$ medulloblastoma models and potential ways to overcome the resistance. We demonstrated that tumors employ distinct mechanisms to evade Smo inhibition such as amplification of Gli2, mutations of Smo as well as upregulation of PI3K signaling. It should be noted that we currently cannot distinguish if the resistance is due to the drug-mediated selection of pre-existing resistant subpopulations or the consequence of a drug-induced changes that renders cells resistant.

Gli2, a key mediator of Hh signaling downstream of Smo (13), was amplified in about 50% of resistant *Ptch*$^{+/-}$*p53*$^{-/-}$ tumors and 20% of resistant *Ptch*$^{+/-}$ tumors and was able to drive resistant tumor growth. It is possible that the genomic instability induced by p53 loss contributes to the increased frequency of Gli2 amplification in *Ptch*$^{+/-}$*p53*$^{-/-}$. Gli2 amplification has been observed in human medulloblastoma (18), albeit at low frequency, and it remains to be seen if Gli2 amplification will be more frequently observed in

medulloblastoma patients that develop resistance to Smo antagonists. Mutations in Smo resulting in loss of sensitivity to NVP-LDE225 constituted another mechanism of resistance and were detected in about 5% of resistant tumors in our study. It should be noted that Gli2 amplification and Smo mutation seemed largely mutually exclusive. Recently, a mutation in Smo (D473H) was identified in a medulloblastoma patient that developed resistance to the Smo antagonist GDC0449 (12,17). The D473H mutation rendered Smo resistant to inhibition by GDC0449. A corresponding mutation in mouse Smo (D477G) was subsequently identified in a $Ptch^{+/-}p53^{-/-}$ mouse tumor that became resistant to GDC0449 in a subcutaneous allograft model suggesting that the mouse model might have value in predicting resistance mechanisms for the human setting. Mutations identified in our study differed from the D477G mutation suggesting that various mutations can render Smo resistant to antagonists. Moreover, it is highly likely that the mutation spectrum and frequency will differ depending on the antagonist used. In the future, the extent of cross-resistance will be important to understand and will help inform whether treatment failure on one SMO inhibitor can be rescued by a structurally distinct inhibitor.

Unexpectedly, we identified upregulation of Igf-1R/PI3K signaling as another potential resistance mechanism by profiling of gene expression changes in resistant versus sensitive tumors. The importance of the compensatory upregulation of this pathway was demonstrated by the ability to overcome the emergence of resistance by combining the Smo antagonist NVP-LDE225 with PI3K/Tor inhibitors. While the underlying mechanism of Igf-1R/PI3K pathway upregulation in resistant tumors awaits further investigation, examination of the CGH data did not reveal overt genetic alterations such as deletion of *Pten* or amplification of *Pi3k* or *Akt* alleles. However, increased expression of IGF2 and its receptor were observed in the majority of the resistant tumors. In this context, it is of interest that Igf-1R and Hh signaling appear to synergize in promoting proliferation of cerebellar neuronal precursors and the formation of medulloblastoma tumors (19–21), and that Igf2 is required for the progression to advanced medulloblastoma in $Ptch^{+/-}$ mice (22). Moreover, a recent study demonstrated that Igf2, through PI3K signaling, potentiates Gli activation induced by low levels of Hh ligand (23). It is possible that under conditions of continuous Hh pathway inhibition, the Igf-1R/PI3K pathway compensates for the loss of Hh signaling and thus becomes a major mediator of resistant tumor growth. In how far this occurs in synergy with residual levels of Hh activity or promotes the expansion of clones that acquired Gli2 amplifications, Smo mutations or other genetic or epigenetic changes needs to be further explored. In this context it is of interest that the upfront concurrent administration of PI3K inhibitors with Smo antagonists was more effective in preventing resistance compared to treatment of established NVP-LDE225 resistant tumors with NVP-BKM120 which only resulted in modest but not statistically significant tumor growth inhibition (data not shown).

In summary, these data indicate that the combination of Smo antagonists with modulators of the PI3K/mTor pathway constitutes a potential strategy to delay or prevent resistance to Smo antagonists and has important implications for future treatment strategies in medulloblastoma and other Smo-dependant human cancers.

Material and Methods

Medulloblastoma allograft studies

Tumors derived from $Ptch^{+/-}p53^{-/-}$ and $Ptch^{+/-}Hic^{+/-}$ transgenic mice were serially passaged as fragments in nude mice. For efficacy studies tumor fragments were dissociated into single cells and 5×10^6 cells were allografted into nude mice and treated with small molecule inhibitors as previously described (5,24). Tumor volumes were measured three times a week and calculated using the ellipsoid formula: (length × width^2)/2. NVP-LDE225 was formulated as diphosphate salt in 0.5% Methylcellulose and 0.5% Tween 80 (Fisher),

NVP-BKM120 in 0.5% Methylcellulose, NVP-BEZ235 in 1 volume of NMP (1-methyl-2-pyrrolidone, Sigma-Aldrich) and 9 volumes of PEG300 (Sigma-Aldrich), and RAD001 in water. Doses are expressed as free-base equivalents. Tumors were harvested for analysis 4 h after the last dose. All animal studies were carried out according to the Novartis Guide for the Care and Use of Laboratory Animals.

Ex-vivo medulloblastoma assay

Tumors were minced and a single cell suspension was prepared using the Papain dissociation system (Worthing Biochemical Co) as previously described (10). Cells were resuspended in serum-free Neurobasal medium (with B27 supplement) (Invitrogen) and plated in 96-well plates at a density of 3×10^5 cells/well in 200 ul medium. Serial dilutions of inhibitors were prepared in DMSO and added at 1 μl per well. Cells were incubated for 48 hours and [^{3}H]-thymidine was added for the last 8 hours to assess cell proliferation. Incorporated radioactivity was quantified as previously described (10). siRNA transfections with scrambled siRNAs (ON-TARGETplus Non-targeting Pool, Dharmacon) and mGli2 siRNAs (Gli2 SiGENOME, Dharmacon) were applied using the DharmaFECT1 transfection reagent according to the manufacturer's instructions (Dharmacon).

Immunoblot analysis

Cell lysates were prepared and analyzed by immunoblot for phospho-S6 (S235/236), total S6, phospho-4EBP1 (T37/46) and total 4EBP1 (CST #2211, 2217, 2855 and 9452, respectively) as described (25)

Smo binding and cell-based assays

Agonist displacements assays and TM3-Gli-luciferase assays were performed as previously described (24). HEPM cells (ATCC #CRL-1486) were cultured in Minimum Essential Medium (Gibco) supplemented with 10% FCS. Cells were plated at 5×10^4 cells/well in 96-well plates and stimulated with recombinant SHH (R&D systems 1845-SH) for 48 h in the presence of serial dilutions of NVP-LDE225. Gli1 mRNA levels were determined at the end of the assay as described below. Smo point mutations were introduced into pcDNA3.1 containing HA-tagged Smo using the QuickChange Lightning Site-directed mutagenesis kit (Strategene). Wild-type and mutant smo constructs were transiently expressed in C3H10T1/2 (ATCC #CCL-226) with a Gli-luciferase reporter and pRL-TK expressing renilla luciferase using GeneJuice transfection reagent as described (12). Serial dilutions of NVP-LDE225 (0.001 to 10 μM final concentration in assay) were added 24 hours after transfection. Firefly and renilla luciferase activity was detected after an additional 24 h with the Dual-Luciferase reporter assay system (Promega). Percent inhibition was calculated relative to DMSO control.

Gene expression analysis

RNA isolation from tumors, cDNA synthesis and real-time quantitative PCR for *Gli1* were performed as described (24). PCR probes used: *mGli1*: Mm494646m1 *mGli2* Mm01293117m1,, *mPtch1:* Mm00436026m1, *mPtch2*: Mm00436047m1, *mCyclinD1*: Mm00432359m1 (Applied Biosystems).

Generation of labelled cDNA and hybridization to 430_2 murine arrays (Affymetrix) were performed as described (26). Expression values were normalized using the Affymetrix MAS5.0 algorithm. Probe sets with MAS5.0 expression below 100 in 90% of samples were excluded from analysis. The remaining probe sets were compared with the pattern in Figure 2A using a Spearman rank correlation, and tested for differential expression as in Figure 3A using a homoscedastic t-test. Using the gene selection methods above, probesets with

nominal p-values <0.01 were assessed for membership in gene sets (transcription factor sets and canonical pathways) extracted from the GeneGo Metacore database (11). Significance values were calculated using a Fisher's Exact test and Benjamini-Hochberg FDR correction (27). Genes with multiple probesets were considered for set membership if any constituent probesets met the selection criteria. Mouse genes were converted to human homologs using the NCBI homologene database, August 2009 build (http://www.ncbi.nlm.nih.gov/homologene).

DNA copy number and sequence analysis

Genomic DNA was extracted from tumors using the DNeasyBlood and Tissue kit (Qiagen) and subjected to copy number analysis with the Agilent Mouse CGH 244K array containing 244,000 features with a median probe spacing of 7.8 Kb per manufacter's instructions. The data was analyzed using the Agilent G4175AA CGH

Analytics 3.4 software for copy number alterations. Genomic copy number for Gli1, Gli2 or Gli3 was determined using custom designed quantitative PCR reagents synthesized by Applied Biosystems (Gli1: forward primer CATTGCCTTTTCTCCTTGTCATCTG, reverse primer GGCGGTCCAGGGAGACT, probe CACCTGTGTCTCGCCGTC; Gli2: forward primer CCCGTGGGTCTTCTCTCTGA, reverse primer GACAGGGCTGCCACTTAGG, probe CCTCCACAGGCCTCC; Gli3: forward primer CTCATCTTTTCCCTGCCTTCCA, reverse primer ACATGTAATGGAGGAATAGGAGATGGA, probe CCTCATGATGTCTGGCATC). qPCR was carried out in 384-well plate and run with the 7900HT Fast Real-Time PCR System (Applied Biosystems) using the default cycling method (50°C for 2 minutes, 95°C for 10 minutes followed by 40 cycles at 95°C for 15 seconds and 60°C for 1 minute). The reaction volume was 12 ul and the mixture included 900 nM of each primer, 250 nM of probe, 1X taqman universal master mix (containing PCR buffer, nucleotides and Taq DNA polymerase) and 10 ng genomic DNA template. Copy numbers were calculated with 6 replicates reactions for each DNA sample with a standard curve constructed with four replicates of 4-fold serial dilution of normal genomic DNA template, ranging from 40 ng to 0.04 ng. Copy number was calculated as $2(T_{DNA}/C_{DNA})$ where T_{DNA} and C_{DNA} are the calculated amount of test gene DNA at the recorded Ct for tumor and calibrator respectively. Copy number data for Gli2 was normalized to Gli3 using the formula $2(T_{dna}/L_{dnaT})/(C_{dna}/L_{dnaC})$ where T_{dna} and C_{dna} represent the amount of Gli2 calculated amount DNA in the tumor and calibrator respectively and L_{dnaT} and L_{dnaC} are the corresponding amount of their Gli3 DNA at the recorded Ct values. Mutation analysis was performed by sequencing of PCR-amplified exon sequences of Smo at Agencourt.0

Supplementary Material

Refer to Web version on PubMed Central for supplementary material.

Acknowledgments

We wish to thank Nicole Hartmann & Frank Staedtler in the Genomics & Genetics Applications core group in Novartis Institutes for Biomedical Research for performing the expression profiling; Ed Lobenhofer and Angel Field at Cogenics Inc. for the CGH profiling. We thank Rosalind Segal for providing *Ptch*$^{+/-}$*p53*$^{-/-}$ tumors and Rebecca Mosher for histopathology support. D.N.W. was supported by NIH/NINDS R01 NS054085-01A1.

Reference List

1. Varjosalo M, Taipale J. Hedgehog: functions and mechanisms. Genes & Development. 2008; 22:2454–2472. [PubMed: 18794343]
2. Toftgard R. Hedgehog signalling in cancer. Cellular and Molecular Life Sciences. 2000; 57:1720–1731. [PubMed: 11130178]

3. Romer JT, Kimura H, Magdaleno S, Sasai K, Fuller C, Baines H, Connelly M, Stewart CF, Gould S, Rubin LL, Curran T. Suppression of the Shh pathway using a small molecule inhibitor eliminates medulloblastoma in Ptc1(+/−)p53(−/−) mice. Cancer Cell. 2004; 6:229–40. [PubMed: 15380514]
4. Engelman JA, Settleman J. Acquired resistance to tyrosine kinase inhibitors during cancer therapy. Current Opinion in Genetics & Development. 2008; 18:73–79. [PubMed: 18325754]
5. Pan, S.; Wu, X.; Jiang, J.; Gao, W.; Wan, Y.; Cheng, D.; Han, D.; Liu, J.; Englund, NP.; Wang, Y.; Peukert, S.; Miller-Moslin, K.; Yuan, J.; Guo, R.; Matsumoto, M.; Vattay, A.; Jiang, Y.; Tsao, J.; Sun, F.; Pferdekamper, AC.; Dodd, S.; Tuntland, T.; Maniara, W.; Kelleher, JF.; Yao, Ym; Warmuth, M.; Williams, J.; Dorsch, M. ACS Medicinal Chemistry Letters. 2010. Discovery of NVP-LDE225, a Potent and Selective Smoothened Antagonist.
6. Frank-Kamenetsky M, Zhang X, Bottega S, Guicherit O, Wichterle H, Dudek H, Bumcrot D, Wang FY, Jones S, Shulok J, Rubin LL, Porter JA. Small-molecule modulators of Hedgehog signaling: identification and characterization of Smoothened agonists and antagonists. J Biol. 2002; 1:10. [PubMed: 12437772]
7. Wetmore C, Eberhart DE, Curran T. Loss of p53 but not ARF accelerates medulloblastoma in mice heterozygous for patched. Cancer Res. 2001; 61:513–6. [PubMed: 11212243]
8. Yauch RL, Gould SE, Scales SJ, Tang T, Tian H, Ahn CP, Marshall D, Fu L, Januario T, Kallop D, Nannini-Pepe M, Kotkow K, Marsters JC, Rubin LL, de Sauvage FJ. A paracrine requirement for hedgehog signalling in cancer. Nature. 2008; 455:406–U61. [PubMed: 18754008]
9. Briggs KJ I, Corcoran-Schwartz M, Zhang W, Harcke T, Devereux WL, Baylin SB, Eberhart CG, Watkins DN. Cooperation between the Hic1 and Ptch1 tumor suppressors in medulloblastoma. Genes & Development. 2008; 22:770–785. [PubMed: 18347096]
10. Oliver TG, Read TA, Kessler JD, Mehmeti A, Wells JF, Huynh TTT, Lin SM, Wechsler-Reya RJ. Loss of patched and disruption of granule cell development in a pre-neoplastic stage of medulloblastoma. Development. 2005; 132:2425–2439. [PubMed: 15843415]
11. Ekins S, Nikolsky Y, Bugrim A, Kirillov E, Nikolskaya T. Pathway mapping tools for analysis of high content data. Methods Mol Biol. 2007; 356:319–350. [PubMed: 16988414]
12. Yauch RL, Dijkgraaf GJP, Alicke B, Januario T, Ahn CP, Holcomb T, Pujara K, Stinson J, Callahan CA, Tang T, Bazan JF, Kan Z, Seshagiri S, Hann CL, Gould SE, Low JA, Rudin CM, de Sauvage FJ. Smoothened Mutation Confers Resistance to a Hedgehog Pathway Inhibitor in Medulloblastoma. Science. 2009; 326:572–574. [PubMed: 19726788]
13. Kasper M, Regl G, Frischauf AM, Aberger F. Gli transcription factors: Mediators of oncogenic Hedgehog signalling. European Journal of Cancer. 2006; 42:437. [PubMed: 16406505]
14. Maira SM, Stauffer F, Brueggen J, Furet P, Schnell C, Fritsch C, Brachmann S, Chene P, De Pover A, Schoemaker K, Fabbro D, Gabriel D, Simonen M, Murphy L, Finan P, Sellers W, Garcia-Echeverria C. Identification and characterization of NVP-BEZ235, a new orally available dual phosphatidylinositol 3-kinase/mammalian target of rapamycin inhibitor with potent in vivo antitumor activity. Molecular Cancer Therapeutics. 2008; 7:1851–1863. [PubMed: 18606717]
15. Voliva, CF.; Pecchi, S.; Burger, M.; Nagel, T.; Schnell, C.; Fritsch, C.; Brachmann, S.; Menezes, D.; Knapp, M.; Shoemaker, K.; Wiesmann, M.; Huh, K.; Zaror, I.; Dorsch, M.; Sellers, WR.; Garcia-Echeverria, C.; Maira, M. Biological characterization of NVP-BKM120, a novel inhibitor of phosphoinositide 3-kinase in phase I/II clinical trials., abstr. Proceedings of the 101st Annual Meeting of the American Association for Cancer; 2010 Apr 17–21; Washinton, DC. 2010. p. 1091Abstract nr 4498. 51
16. Tremblay MR, Nesler M, Weatherhead R, Castro AC. Recent patents for Hedgehog pathway inhibitors for the treatment of malignancy. Expert Opinion on Therapeutic Patents. 2009; 19:1039–1056. [PubMed: 19505195]
17. Rudin CM, Hann CL, Laterra J, Yauch RL, Callahan CA, Fu L, Holcomb T, Stinson J, Gould SE, Coleman B, LoRusso PM, Von Hoff DD, de Sauvage FJ, Low JA. Brief Report: Treatment of Medulloblastoma with Hedgehog Pathway Inhibitor GDC-0449. New England Journal of Medicine. 2009; 361:1173–1178. [PubMed: 19726761]
18. Northcott PA, Nakahara Y, Wu XC, Feuk L, Ellison DW, Croul S, Mack S, Kongkham PN, Peacock J, Dubuc A, Ra YS, Zilberberg K, Mcleod J, Scherer SW, Rao JS, Eberhart CG, Grajkowska W, Gillespie Y, Lach B, Grundy R, Pollack IF, Hamilton RL, Van Meter T, Carlotti CG, Boop F, Bigner D, Gilbertson RJ, Rutka JT, Taylor MD. Multiple recurrent genetic events

converge on control of histone lysine methylation in medulloblastoma. Nature Genetics. 2009; 41:465–472. [PubMed: 19270706]

19. Hartmann W, Wiestler OD, Schilling K, Pietsch T. IGF-II is a growth factor for medulloblastoma cells and cerebellar progenitor cells. Neuro-Oncology. 2004; 6:408.
20. Kenney AM, Widlund HR, Rowitch DH. Hedgehog and PI-3 kinase signaling converge on Nmyc1 to promote cell cycle progression in cerebellar neuronal precursors. Development. 2004; 131:217–228. [PubMed: 14660435]
21. Rao G, Pedone CA, Del Valle L, Reiss K, Holland EC, Fults DW. Sonic hedgehog and insulin-like growth factor signaling synergize to induce medulloblastomaformation from nestin-expressing neural progenitors in mice. Oncogene. 2004; 23:6156–6162. [PubMed: 15195141]
22. Corcoran RB, Raveh TB, Barakat MT, Lee EY, Scott MP. Insulin-like Growth Factor 2 Is Required for Progression to Advanced Medulloblastoma in patched1 Heterozygous Mice. Cancer Research. 2008; 68:8788–8795. [PubMed: 18974121]
23. Riobo NA, Lu K, Ai XB, Haines GM, Emerson CP. Phosphoinositide 3-kinase and Akt are essential for Sonic Hedgehog signaling. Proceedings of the National Academy of Sciences of the United States of America. 2006; 103:4505–4510. [PubMed: 16537363]
24. Miller-Moslin K, Peukert S, Jain RK, Mcewan MA, Karki R, Llamas L, Yusuff N, He F, Li YH, Sun YC, Dai M, Perez L, Michael W, Sheng T, Lei HS, Zhang R, Williams J, Bourret A, Ramamurthy A, Yuan J, Guo RB, Matsumoto M, Vattay A, Maniara W, Amaral A, Dorsch M, Kelleher JF. 1-Amino-4-benzylphthalazines as Orally Bioavailable Smoothened Antagonists with Antitumor Activity. Journal of Medicinal Chemistry. 2009; 52:3954–3968. [PubMed: 19469545]
25. Wee S, Wiederschain D, Maira SM, Loo A, Miller C, DeBeaumont R, Stegmeier F, Yao YM, Lengauer C. PTEN-deficient cancers depend on PIK3CB. Proceedings of the National Academy of Sciences of the United States of America. 2008; 105:13057–13062. [PubMed: 18755892]
26. Wiederschain D, Chen L, Johnson B, Bettano K, Jackson D, Taraszka J, Wang YK, Jones MD, Morrissey M, Deeds J, Mosher R, Fordjour P, Lengauer C, Benson JD. Contribution of polycomb homologues Bmi-1 and Mel-18 to medulloblastoma pathogenesis. Molecular and Cellular Biology. 2007; 27:4968–4979. [PubMed: 17452456]
27. Hochberg Y, Benjamini Y. More Powerful Procedures for Multiple Significance Testing. Statistics in Medicine. 1990; 9:811–818. [PubMed: 2218183]

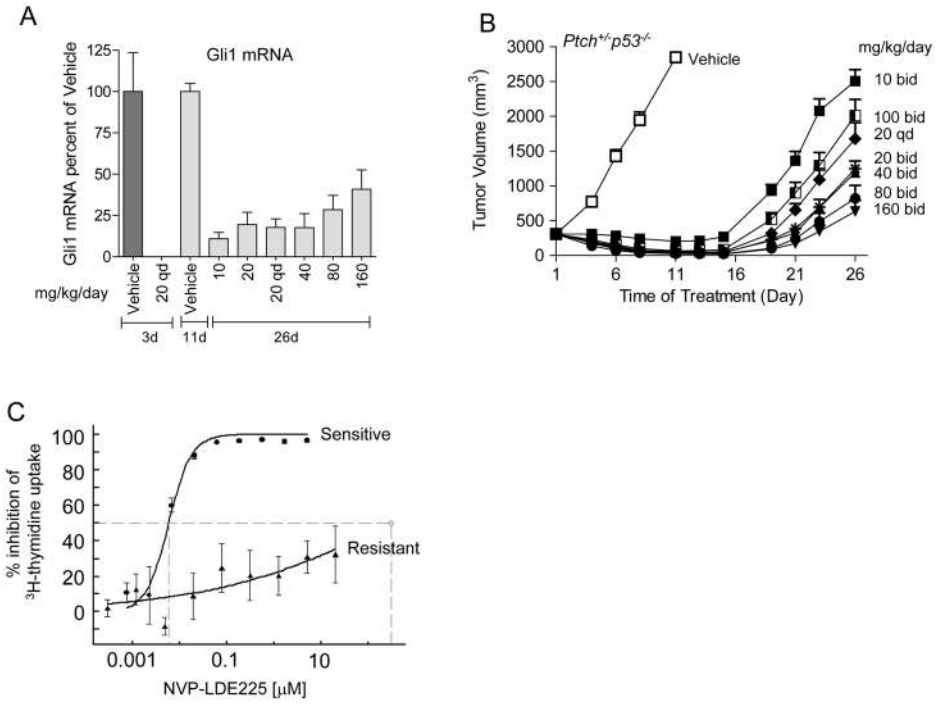

Figure 1. Antagonism of Smo inhibits Hh signaling and growth of *Ptch*$^{+/-}$*p53*$^{-/-}$ tumors, but induces resistance

Nude mice subcutaneously implanted with medulloblastoma tumors were treated with vehicle (control) or NVP-LDE225 at different doses (indicated in mg/kg/day once a day (qd) or split in two doses (bid)). (**A**) Gli1 mRNA levels in tumors quantified at day 3 (black) or day 26 (gray, vehicle control taken on day 11 when tumor size limit was reached) post treatment, normalized to β-actin and blotted as % of matching vehicle for the respective study, and tumor volume over time (**B**) are shown. Data are expressed as mean ± s.e.m, (n=8). **C,** NVP-LDE225 inhibits proliferation of sensitive tumors (filled circles) but not of resistant tumors cells ex-vivo (filled triangles) at low nM concentration, as measured *in vitro* by ^{3}H-thymidine uptake. Data expressed as mean ± s.d, (n=3). Results are shown for one sensitive and one resistant tumors but similar results were obtained for multiple different tumors.

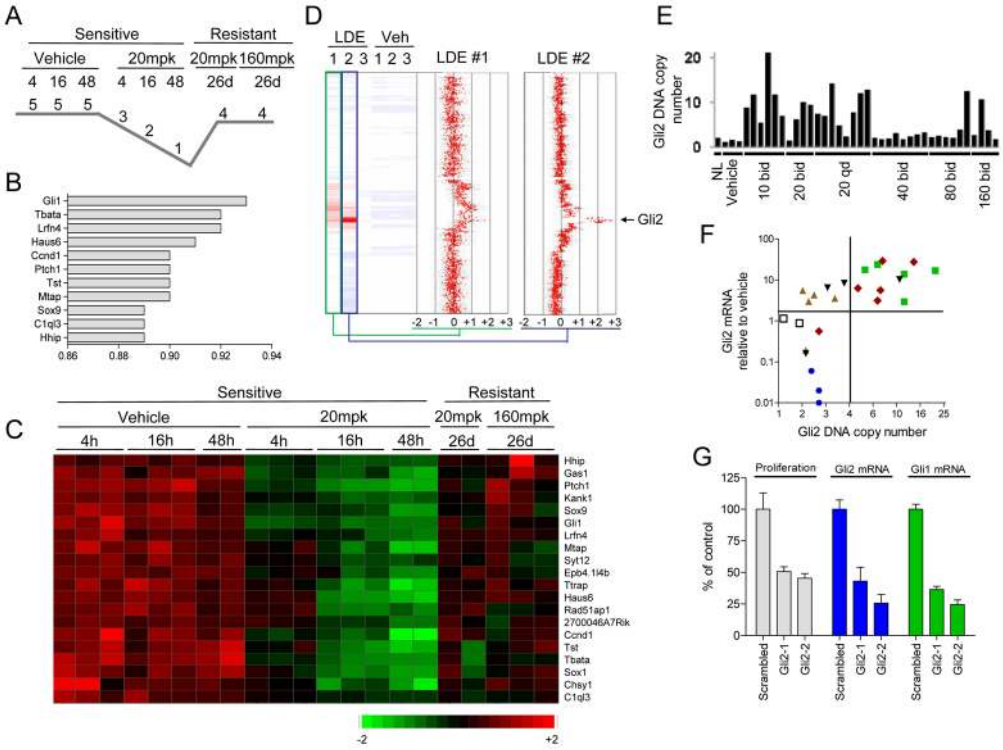

Figure 2. Smo resistant *Ptch*$^{+/-}$*p53*$^{-/-}$ tumors acquire Gli2 amplifications and are sensitive to Gli2 inhibition

RNA from sensitive tumors treated with either vehicle or NVP-LDE225 (20mg/kg/day) for 4, 16 and 48 hours, and resistant tumors treated with 20 or 160 mg/kg/day (mpk) for 26 days (d) was profiled on Affymetrix mouse gene expression arrays. **A**, Pattern of genes initially inhibited by NVP-LDE225 but reemerging in resistant tumors. Numbers express relative rank in expression. **B**, Top ranking genes by Spearman correlation of expression matching with the pattern in 2A. **C,** Heat map of the top ranked genes associated with the pattern in 2A. Each gene's expression values are z-transformed for comparability, with red indicating relatively high expression and green indicating relatively low expression. **D**, CGH analysis using the Agilent Mouse Genome CGH Microarray Kit 244A of three resistant (LDE 1,2,3) and three sensitive (Veh 1,2,3) tumors identified a focal amplification in the region containing Gli2 on Chromosome 1 in 2 out of 3 resistant tumors. Copy number changes are expressed as log2. **E**, Additional DNA from normal liver (NL), vehicle (controls) and resistant tumors was analyzed by quantitative PCR for the Gli2 locus. **F**, Correlation between levels of Gli2 mRNA expression and Gli2 copy number is shown for vehicle-treated control tumors (open square) and resistant tumors that emerged after treatment with NVP-LDE225 at 10 bid (green square), 20 qd (red diamond), 40 bid (brown triangle), 80 bid (blue circle) and 160 bid (black inverse triangle) mg/kg/day. Axis in log10 scale. **G**, Inhibition of Gli2 mRNA levels by siRNA knock-down of Gli2 was associated with decreased proliferation and Gli1 mRNA expression in resistant Gli2 amplified (copy number:20) and Gli2-overexpressing (17-fold) medulloblastoma tumors. Two independent Gli2 siRNAs (Gli2-1 and Gli2-1) were used.

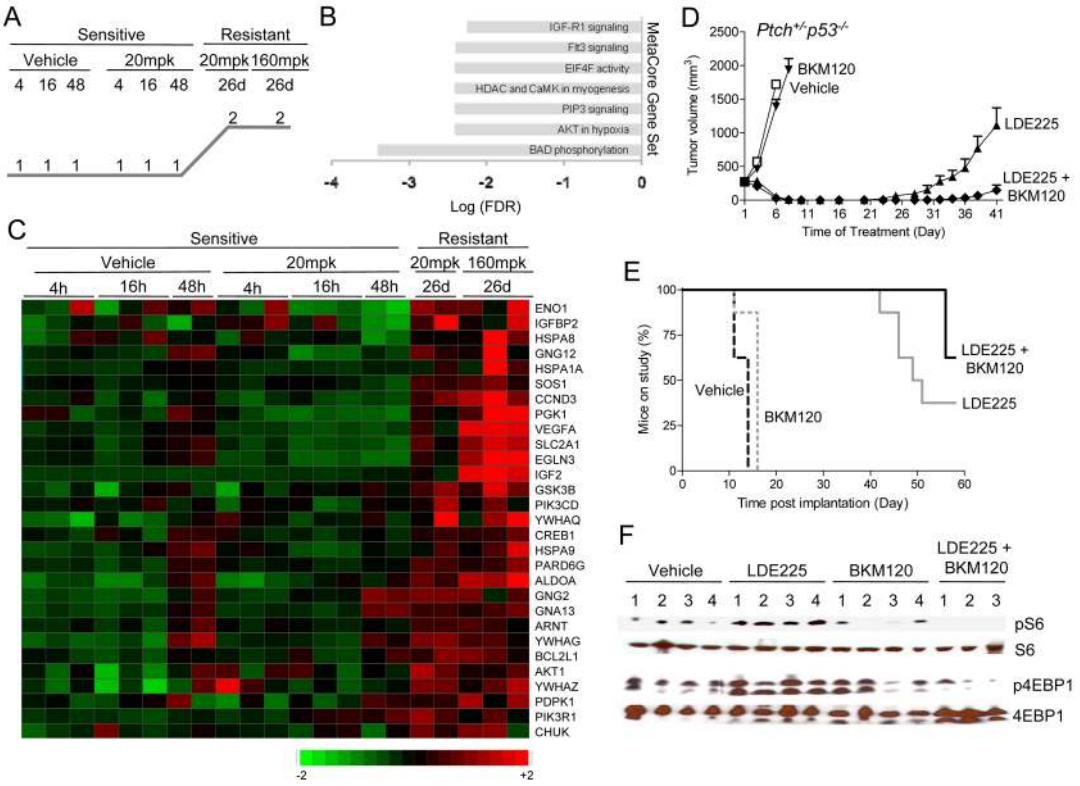

Figure 3. The PI3K/mTor pathway is upregulated in NVP-LDE225 resistant *Ptch*$^{+/-}$*p53*$^{-/-}$ tumors, and emergence of resistance is delayed by combination treatment with the Smo and PI3K inhibitors, NVP-LDE225 and NVP-BKM120

A, Affymetrix gene expression data were mined for genes not affected by short-term NVP-LDE225 treatment, but upregulated in resistant tumors. **B,** Pathway categories upregulated in resistant tumors ranked by FDR scores **C,** Heat map of expression values of upregulated genes inAkt, PIP3 and Igf-1R pathway category.. Data normalized as in Fig. 2C. **D,E** Nude mice subcutaneously implanted with *Ptch*$^{+/-}$*p53*$^{-/-}$ tumors were treated with vehicle (control), NVP-LDE225 (80mg/kg/day qd), NVP-BKM120 (30mg/kg/day qd) or NVP-LDE225 in combination with NVP-BKM120 at the same doses and schedules starting on day 9 post-implant. Tumor volume (mean ± s.e.m. (n=8)) (**D**) and time to end point (tumor volume reaching 700 mm^3) (**E**) are shown.. **F,** Total protein isolated from tumors at the end of the study was evaluated for phospho-S6 (S235/236), phospho-4EBP1 (T37/36) and total S6 and 4EPB1.

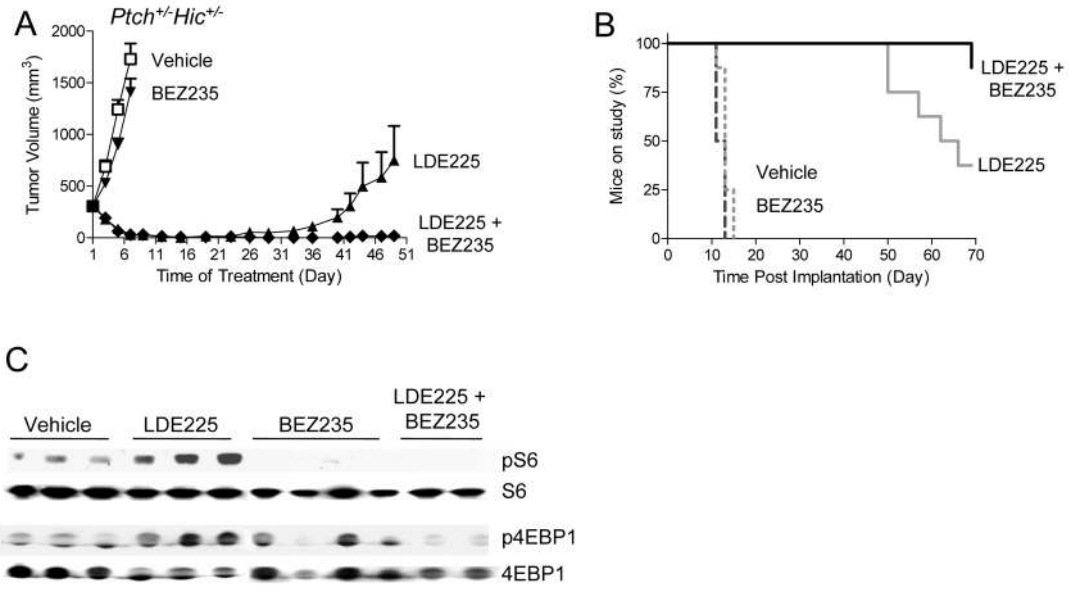

Figure 4. The emergence of resistance in *Ptch*$^{+/-}$*Hic*$^{+/-}$ tumors is suppressed by combination treatment with the Smo and PI3K/mTor inhibitors, NVP-LDE225 and NVP-BEZ235

A, Nude mice subcutaneously implanted with *Ptch*$^{+/-}$*Hic*$^{+/-}$ tumors were treated with vehicle (control), NVP-LDE225 (80mg/kg/day qd), NVP-BEZ235 (40mg/kg/day qd) or NVP-LDE225 in combination with NVP-BEZ235 at the same doses and schedules starting on day 8 post-implant. Tumor volume (mean ± s.e.m. (n=8)) (A) and time to end point (tumor volume reaching 700 mm^3) (**B**) are shown. **C)**, Total protein isolated from tumors at the end of the study was evaluated for phospho-S6 (S235/236), phospho-4EBP1 (T37/36) and total S6 and 4EPB1.

Table 1

Mutations rendering Smo resistant to inhibition by NVP-LDE225

Mouse Smo	Number of tumors with mutation*	Model mutation was identified	LDE225 IC50 [uM]#
Wild-type			0.006
N223D	1	$Ptch^{+/-}p53^{-/-}$	> 10
L225R	2	$Ptch^{+/-}p53^{-/-}$, $Ptch^{+/-}Hic^{+/-}$	> 10
D388N	2	$Ptch^{+/-}Hic^{+/-}$	> 10
S391N	1	$Ptch^{+/-}p53^{-/-}$	> 10
G457S	1	$Ptch^{+/-}p53^{-/-}$	0.4

*out of 135 resistant tumors analyzed

#Inhibition of Smo wild-type or mutant induced Gli-luciferase activity in transient transfection assay in C3H10T1/2 cells (see Supplementary Fig. 4).